Mini Review | Open Access

Energy Materials

Jiang *et al. Energy Mater.* **2026**, *6*, 600082 **DOI:**10.20517/energymater.2026.90

Dendrite formation mechanisms and suppression strategies of zinc-based flow batteries

Yi Jiang[1], Jinze Zhang[1], Meisheng Han[1], Puiki Leung[3], Yubai Li[4], Wenjia Li[1], Bin Liu[1], Qinping Jian[2], Jiayou Ren[2,*], Lei Wei[1,*], Tianshou Zhao[1,2,*]

Keywords:
Zinc-based flow batteries, dendrites, suppression strategies

Citation: Jiang, Y.; Zhang, J.; Han, M.; Leung, P.; Li, Y.; Li, W.; Liu, B.; Jian, Q.; Ren, J.; Wei, L.; Zhao, T. Dendrite formation mechanisms and suppression strategies of zinc-based flow batteries. *Energy Mater.* **2026**, *6*, 600082. https://dx.doi.org/10.20517/energymater.2026.90

Received: 27 Apr 2026 **First Decision:** 27 May 2026 **Revised:** 1 Jul 2026 **Accepted:** 15 Jul 2026 **Published:** 23 Jul 2026

Academic Editor: Jiazhao Wang **Copy Editor:** Fangling Lan **Production Editor:** Fangling Lan

Check for updates

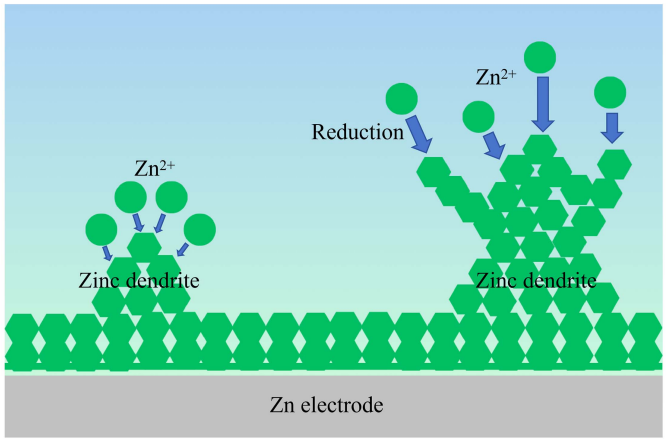

Abstract

Zinc-based flow batteries (ZFBs) are considered a promising energy storage technology because of their high safety, low cost, and high energy density. However, during charging, zinc metal tends to deposit unevenly on the negative electrode, leading to the formation of undesirable dendrites. The growth of these dendrites may pierce the separator, causing internal short circuits or, ultimately, resulting in battery failure. This review explains the mechanisms of zinc dendrite formation and summarizes their adverse effects on battery performance and stability. It then reviews the main strategies currently being explored to suppress dendrite growth, including electrolyte optimization and modifications to electrodes and separators. Finally, the review provides an outlook on the future of dendrite suppression strategies for ZFBs.

[1]SUSTech Energy Institute for Carbon Neutrality, Department of Mechanical and Energy Engineering, Southern University of Science and Technology, Shenzhen 518055, Guangdong, China.
[2]Department of Mechanical and Aerospace Engineering, The Hong Kong University of Science and Technology, Clear Water Bay, Kowloon, Hong Kong, China.
[3]Key Laboratory of Low-Grade Energy Utilization Technologies and Systems, MOE, Chongqing University, Chongqing 400030, China.
[4]Key Laboratory of Ocean Energy Utilization and Energy Conservation of Ministry of Education, Dalian University of Technology, Dalian 116023, Liaoning, China.

***Correspondence to:** Dr. Jiayou Ren, Department of Mechanical and Aerospace Engineering, The Hong Kong University of Science and Technology, Clear Water Bay, Kowloon, Hong Kong, China. E-mail: jrenai@connect.ust.hk; Dr. Lei Wei, SUSTech Energy Institute for Carbon Neutrality, Department of Mechanical and Energy Engineering, Southern University of Science and Technology, Shenzhen 518055, Guangdong, China. E-mail: weil@sustech.edu.cn; Dr. Tianshou Zhao, SUSTech Energy Institute for Carbon Neutrality, Department of Mechanical and Energy Engineering, Southern University of Science and Technology, Shenzhen 518055, Guangdong, China; Department of Mechanical and Aerospace Engineering, The Hong Kong University of Science and Technology, Clear Water Bay, Kowloon, Hong Kong, China. E-mail: metzhao@ust.hk

INTRODUCTION

Today, the world is undergoing an accelerated transition toward carbon neutrality, accompanied by a steady rise in renewable power generation[1]. By 2025, the global installed capacity of solar power had surpassed that of coal-fired power, while wind power had exceeded that of hydropower and other renewable sources[2]. It is projected that, by 2050, wind and solar energy will dominate global electricity generation[3,4]. However, the intermittent and variable nature of wind and solar power impedes their large-scale integration into the grid, posing a major engineering challenge[5,6]. Fortunately, various energy storage technologies have emerged, including pumped hydro storage[7], compressed air energy storage[8], and electrochemical energy storage[9]. Among these, pumped hydro storage is currently the most widely deployed and has the largest installed capacity[10]. However, its strong dependence on geographical conditions and water resources limits its broader application[7]. Similarly, compressed air energy storage is constrained by its large land requirements[8]. In contrast, electrochemical energy storage has developed rapidly owing to its high efficiency, flexibility, and scalability[11]. Major electrochemical energy storage technologies include lithium-ion batteries[12,13], sodium-ion batteries[14,15], and flow batteries[16,17], *etc*. Among them, flow battery technology has attracted significant attention due to its flexible design, long cycle life, and inherent safety[18-20].

Among various flow battery technologies, zinc-based flow batteries (ZFBs), particularly zinc-bromine and zinc-iron flow batteries, have attracted considerable attention because of their low cost and high energy density. Zinc is abundant and inexpensive, whereas vanadium is relatively scarce, costly, and vulnerable to supply-chain volatility[21,22]. Accordingly, zinc-based electrolytes are generally more economical than vanadium electrolytes, offering a potential cost advantage for large-scale energy storage. In addition, zinc undergoes a two-electron plating/stripping reaction, whereas vanadium redox couples typically involve single-electron transfer[23]. This reaction mechanism enables zinc-bromine flow batteries to achieve a theoretical specific energy of up to 435 Wh kg^{-1} and practical volumetric energy densities several times higher than those of vanadium redox flow batteries[24,25]. Their higher energy density reduces electrolyte volume and system footprint, making them attractive for distributed, user-side, and residential energy-storage applications. Moreover, in representative zinc-bromine systems, both half-cells initially contain zinc bromide electrolyte[26]. Electrolyte crossover therefore causes less irreversible cross-contamination than in flow batteries employing chemically distinct anolytes and catholytes[27], facilitating electrolyte rebalancing, capacity recovery, and long-term maintenance. The recyclability of zinc-based electrolytes further supports their potential for sustainable energy-storage applications[28,29].

Despite these advantages, the practical deployment of ZFBs remains severely constrained by zinc dendrite growth[30,31] [Figure 1]. During charging, nonuniform Zn^{2+} transport, nucleation, and deposition on the zinc anode can produce protruding deposits that progressively develop into dendrites[32]. These dendrites may penetrate the separator, resulting in internal short circuits and eventual cell failure[30,33]. Dendritic and nonuniform zinc deposition also increases the electrochemically active surface area and can intensify parasitic hydrogen evolution[34], thereby reducing coulombic efficiency, accelerating capacity decay[35], and shortening system lifetime[36]. Zinc dendrites therefore represent a major barrier to the large-scale commercialization of ZFBs[37,38]. In response, a multiscale framework for dendrite suppression has emerged, encompassing electrolyte regulation[32,39,40], anode modification[5,41,42], and separator design[43-45]. However, substantial inconsistencies remain in the proposed suppression mechanisms[35], applicable operating conditions[46], and performance-evaluation criteria[47]. These discrepancies hinder direct comparison among reported strategies and complicate the identification of technically and economically viable engineering solutions[38]. Accordingly, this review elucidates the mechanisms underlying zinc dendrite formation, critically compares the benefits and trade-offs of major suppression strategies, and proposes a more reproducible and comparable evaluation framework together with future research directions.

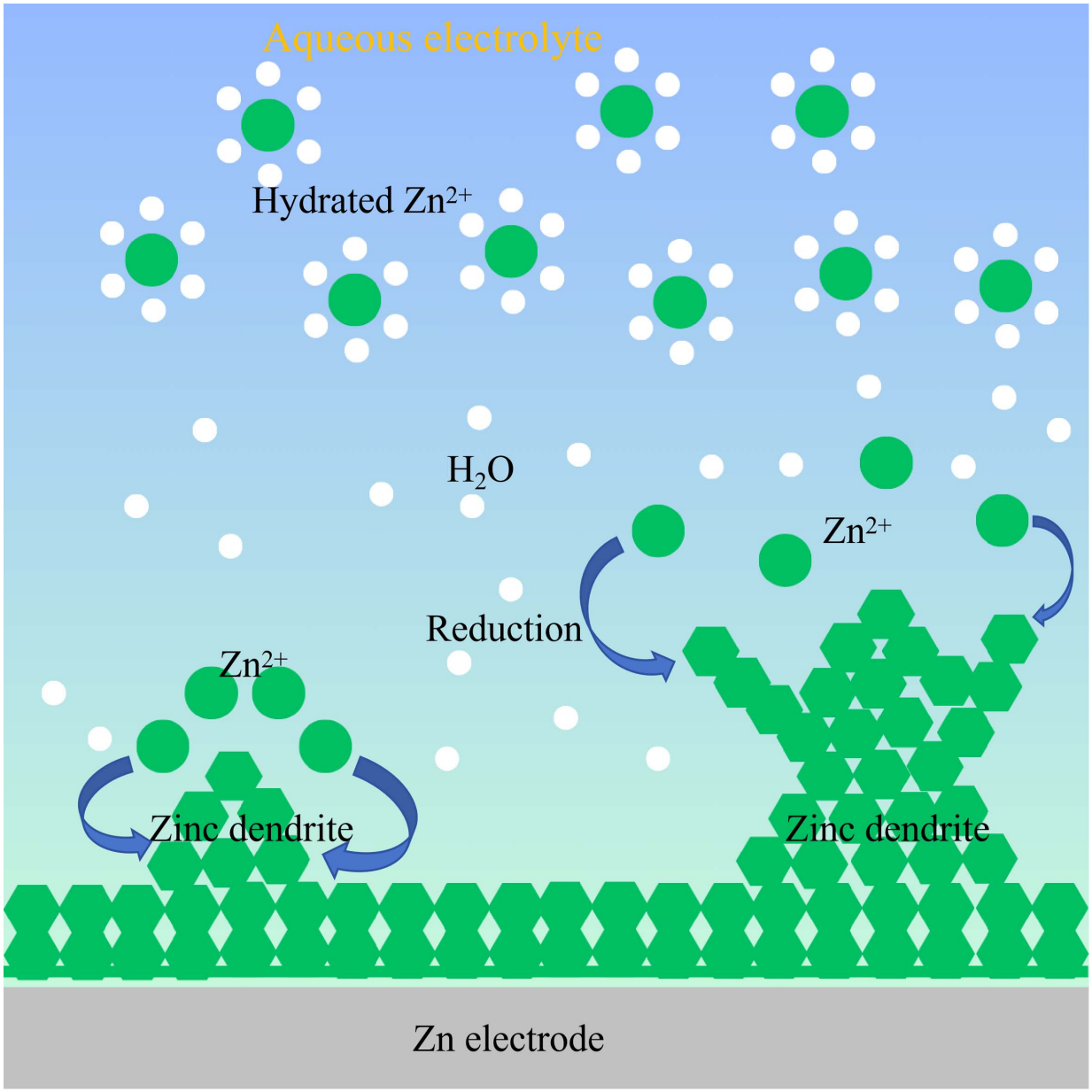

Figure 1. Dendrite growth in a two-dimensional plane.

DENDRITE FORMATION: MECHANISM AND DETRIMENTAL CONSEQUENCES

During charging of ZFBs, Zn^{2+} ions are reduced to metallic zinc on the three-dimensional conductive substrate of the negative electrode[48]. Microscale surface roughness, residual oxides, and exposed carbon-fiber tips can geometrically intensify the local electric field, producing a pronounced tip effect[49]. At high current density, the rapid depletion of Zn^{2+} near the electrode surface induces concentration polarization, causing the deposition process to shift from kinetic to mixed electrochemical-mass-transport control[35]. The resulting increase in overpotential accelerates nucleation kinetics exponentially[50,51], favoring instantaneous nucleation[52] and promoting zinc deposition at surface protrusions with lower nucleation barriers[50,53]. Subsequently, zinc atoms deposit epitaxially along the <10$\bar{1}$0> crystallographic direction of hexagonal close-packed zinc[54], while being continuously driven toward the membrane direction by local pH increase and electric-field gradient[55]. As a result, needle-like or pine tree-like dendrites, typically 50-200 nm in diameter and tens of micrometers in length, are gradually formed[56] [Figure 2]. Meanwhile, parasitic water-reduction

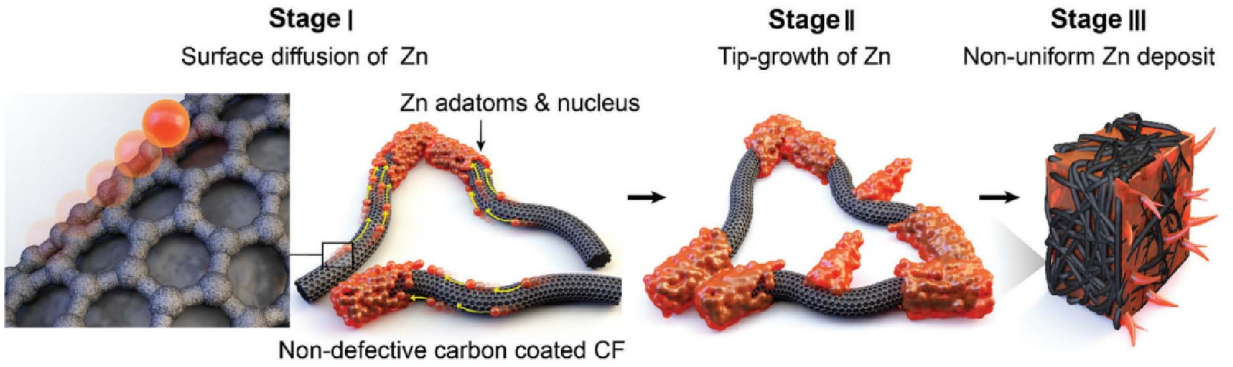

Figure 2. Schematic illustration of zinc aggregation and subsequent nonuniform zinc growth on the non-defective 3-dimensional carbon felt (CF). Reprinted with permission from[33]. Copyright 2020, Royal Society of Chemistry.

reactions generate OH^-, inducing the ZnO-based passivation layers[57]. These heterogeneous deposits exacerbate local electric-field distortion and ultimately establish a self-amplifying growth loop[47,58].

Although the above framework emphasizes electric-field heterogeneity, concentration polarization, and nucleation behavior, the fundamental mechanisms governing zinc dendrite formation remain the subject of debate[59]. Recent studies have increasingly highlighted the roles of ion desolvation and surface diffusion as additional interfacial factors[60]. In aqueous electrolytes, Zn^{2+} ions are typically surrounded by a strongly bound hydration shell, and sluggish desolvation can hinder interfacial charge transfer and produce spatially nonuniform deposition kinetics[61]. After charge transfer, insufficient surface diffusion of adsorbed zinc species may further prevent their redistribution from high-energy protrusions to more stable surface sites, thereby amplifying morphological instability. These findings suggest that dendrite suppression should not rely solely on improving macroscopic ion transport. Regulating interfacial desolvation barriers and surface diffusion pathways may be more effective for suppressing dendrite formation and promoting compact zinc deposition[62].

The formation and continued growth of zinc dendrites have severe consequences for battery performance and safety. Once dendrites penetrate the membrane and come into direct contact with bromine or iron complexes in the positive electrolyte, an internal short circuit can occur, resulting in a sudden drop in cell voltage and a coulombic efficiency approaching zero[30]. In addition, dendrite fracture can generate "dead zinc" particles suspended in the electrolyte, reducing zinc utilization and increasing capacity losses[63]. Moreover, dendrite growth progressively destroys the surface flatness of the negative electrode substrate, rendering subsequent zinc deposition increasingly disordered[64].

Furthermore, dendrite growth and parasitic side reactions mutually reinforce each other. From a thermodynamic standpoint, the spontaneous reaction between zinc and the electrolyte, along with hydrogen evolution during charging, is inherently unavoidable[65]. These parasitic side reactions generate hydrogen gas and deplete the electrolyte, leading not only to capacity fading and reduced energy efficiency but also to increased internal pressure in sealed cells, ultimately shortening cycle life[5,66]. The core approach to inhibiting the hydrogen evolution reaction (HER) involves reducing the activity of water molecules at the anode surface while promoting preferential and homogeneous zinc-ion deposition[67].

As a consequence, due to the growth of dendrites, the cycle life of the system may decrease dramatically, while maintenance costs may increase significantly, thereby severely hindering the large-scale commercial application of ZFBs for energy storage[68].

DENDRITE SUPPRESSION STRATEGIES

To suppress dendrite growth and improve the energy efficiency of ZFBs[31], researchers have developed a variety of strategies targeting different battery components[69]. Current approaches mainly include electrolyte regulation[70], electrode modification[71], and separator optimization[72], *etc*. These strategies can enhance energy efficiency and provide valuable directions for future research[73].

Electrolyte engineering

The electrolyte serves as the ion-conducting medium in ZFBs[74] and provides the active species required for battery operation[75]. A large body of prior research has demonstrated that electrolyte regulation is an effective strategy for suppressing dendrite growth[40,76,77]. By tailoring electrolyte properties, the electrochemical reaction environment can be controlled, thereby suppressing dendrite formation[78]. This approach generally involves either introducing functional additives or directly modifying the electrolyte composition[79]. Reported strategies for electrolyte modification include the addition of hydrophilic solubilizers[70], the use of phosphate salts[80], and the development of liquid metal electrolytes[81].

Hydrophilic solubilizers

Hydrophilic solubilizers are electrolyte additives and are highly effective in zinc acetate electrolytes. Zinc acetate is low-cost and environmentally benign[82], but its poor water solubility limits its practical application[83-85]. To address this issue, a hydrophilic solubilizer composed of potassium acetate, urea, and acetamide at a molar ratio of 10M:10M:8M can replace the hydrophobic solvation sheath with hydrophilic functional groups, thereby converting zinc acetate into a hydrophilic coordination structure. In addition, the extra acetate ions introduced by the hydrophilic solubilizer can partially replace water molecules in the original solvent sheath around zinc ions, changing the coordination mode from bidentate to monodentate, thereby significantly increasing zinc acetate concentration from 1.6 to 23 M[86]. As the zinc ion concentration increases, the electrolyte exhibits higher Zn^{2+} transference numbers and longer Sand's time, which, in turn, enable a higher areal capacity. Sand's time is the time at which the Zn^{2+} concentration at the electrode surface decreases to zero during constant-current deposition[87]. A higher Zn^{2+} concentration also promotes more uniform zinc deposition and lowers the overpotential. Moreover, the hydrophilic solubilizer expands the cathodic and anodic limits, achieving a stable window of approximately 2.5 V. With hydrophilic solubilizers, the deposited zinc maintains a dense and smooth morphology after 400 cycles, owing to high zinc salt concentration and a high Zn^{2+} transference number in the electrolyte, which improve the uniformity of zinc deposition/stripping and effectively suppress dendrite growth. Even after 4,000 cycles, 70% of the initial capacity can still be maintained[70].

Zinc-pyrophosphate complex

In a traditional zinc bromide electrolyte, each zinc ion is coordinated by 6 water molecules [Figure 3A], with the main Zn-O bond peak appearing at 1.99 Å [Figure 3B], readily producing zinc dendrites. The optimized structure of hydrated zinc ion is shown in Figure 3C. In this study, to create a strong coordination environment that promotes uniform zinc deposition and effectively suppresses dendrite growth, zinc chloride was chelated with potassium pyrophosphate to form a zinc-pyrophosphate complex anolyte [Figure 3D]. Under these conditions, a new peak appears at 1.7 Å from the zinc ion [Figure 3E]. The Zn-O coordination number decreases to 4. The optimized structure of zinc pyrophosphate is shown in Figure 3F. In addition, the large anion size and high negative charge can effectively hinder the transport of zinc ions through the cation-exchange membrane, thereby fundamentally preventing zinc-ion migration. Simultaneously, this complex anolyte regulates the thermodynamics of zinc nucleation, thereby enabling dendrite-free dense deposition. The interfacial water activity of $Zn(PPi)_2^{6-}$ ions is effectively reduced, allowing the subsequently dissociated Zn^{2+} ions to plate on the zinc surface in an orderly manner with the

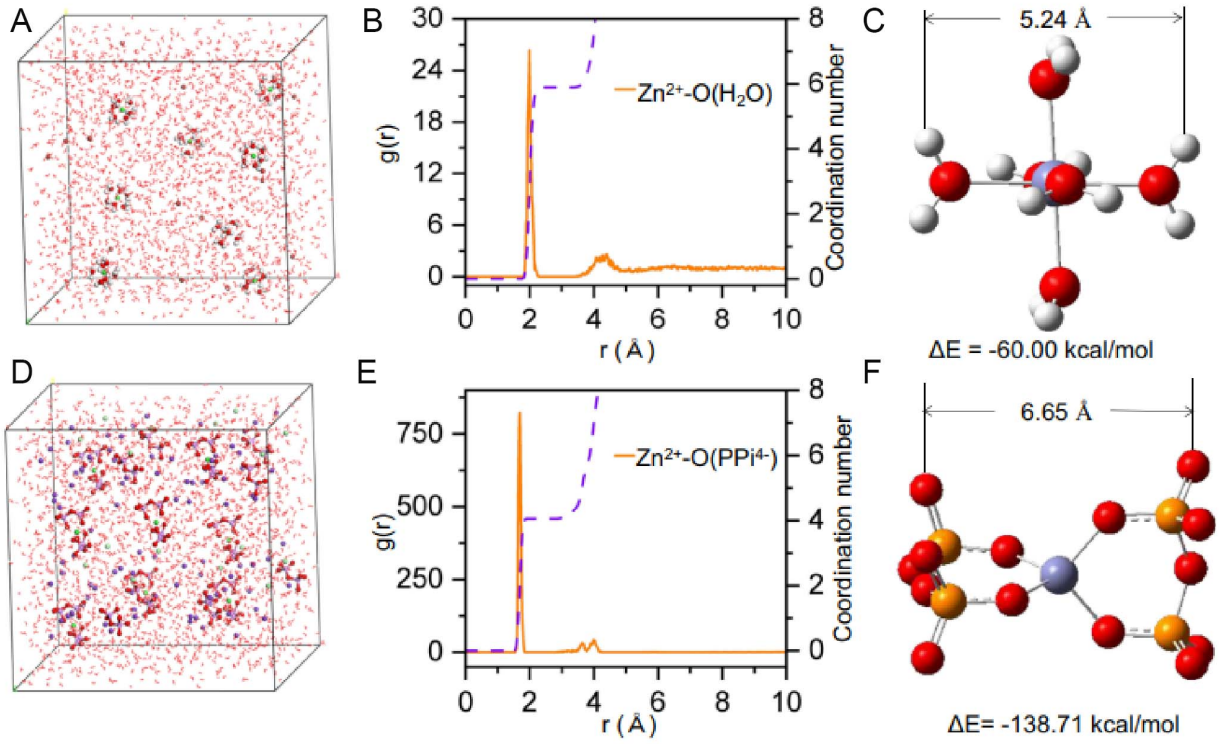

Figure 3. Theoretical calculation results for $Zn(H_2O)_6^{2+}$ and $Zn(PPi)_2^{6-}$. Reprinted from Ref.[80]. 3D snapshot of (A) 0.2 M $ZnBr_2$ system and (D) 0.2 M $ZnCl_2$-K_4PPi (1:3) system obtained from molecular dynamics (MD) simulations. RDFs for (B) $ZnBr_2$ and (E) $ZnCl_2$-K_4PPi system collected from MD simulations. The optimized molecular structures and corresponding binding energies of (C) $Zn(H_2O)_6^{2+}$ and (F) $Zn(PPi)_2^{6-}$.

assistance of the PPi^{4-} ion. Hence, the $Zn(PPi)_2^{6-}$ electrolyte can alleviate the undesired HER and facilitate smooth zinc plating. As a result, the zinc deposition/stripping potential dropped to -1.08 V, while battery voltage increased from 1.29 to 1.61 V, corresponding to a 24% improvement. Even at a high current density of 200 mA cm^{-2}, the battery maintains a capacity retention of over 97% after 250 cycles, and the peak power density reaches 606.5 mW cm^{-2}, far exceeding traditional performance limits of conventional ZFBs[80].

Liquid metal electrolyte

Liquid metals, with low melting points and remaining liquid at or near room temperature, exhibit high fluidity and metallic conductivity[88]. Among them, gallium-based liquid metals (Ga-LMs) are particularly promising due to their low toxicity, intrinsic safety, self-healing properties, and good compatibility with other metallic elements[89]. Furthermore, alloying gallium with tin can further decrease the melting point while reducing costs[90]. The eutectic Ga-In-Sn liquid metal systems can dissolve zinc, transforming from a solid deposited state into a fluid metallic form and eventually forming a eutectic Ga-In-Sn-Zn liquid metal [Figure 4A and B]. The corresponding battery performance is illustrated in Figure 4C. In this system, the conventional solid-liquid zinc deposition/stripping process is effectively converted into a liquid-liquid electrochemical reaction, thereby increasing the areal capacity of the zinc anode and alleviating the limitations associated with solid zinc accumulation. Compared with the porous CF electrode, the LM-based ZFB achieved an ultrahigh areal capacity of up to 640 mAh cm^{-2} (i.e., 16 h of charging and approximately 16 h of discharging), with a high average coulombic efficiency (CE) of 98.4%. Moreover, ZFBs with an LM anode have an extended cycle life exceeding 180 days (4,400 h) at an areal capacity of 120 mAh cm^{-2}[81].

In summary, electrolyte regulation represents a highly effective strategy for suppressing zinc dendrite growth in ZFBs by tailoring the Zn^{2+} solvation structure, ion transport behavior, and zinc deposition

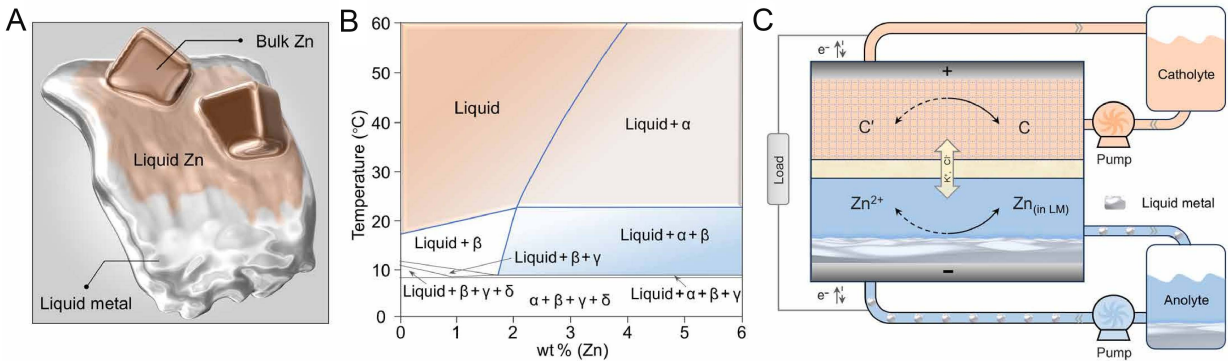

Figure 4. Characteristics of zinc in liquid metal (LM). Reprinted with permission from[81] ,Copyright 2025, The American Association for the Advancement of Science. (A) Schematic of zinc dissolved in LM to form a eutectic alloy at room temperature. (B) Phase diagram of a Zn-LM system. The fixed weight ratios of LM are as follows: 68.5% for Ga, 21.5% for In, and 10.0% for Sn. (C) Schematic of a ZFB assembled with LM. C/C, catholyte in oxidized/reduced state.

thermodynamics. Approaches such as hydrophilic solubilizers, zinc-pyrophosphate complex electrolytes, and liquid-metal electrolytes can improve zinc-ion transference, prolong Sand's time, promote dense and uniform zinc deposition, and mitigate local concentration polarization. In particular, these strategies either stabilize the coordination environment of Zn^{2+} to guide dendrite-free electrodeposition or fundamentally alter the zinc deposition pathway, thereby reducing dendrite formation and enhancing cycling stability. Therefore, electrolyte engineering not only provides an effective means to inhibit zinc dendrites but also offers significant potential to improve the capacity, durability, and practical viability of high-performance ZFBs.

Electrode modification

The electrode provides both electrochemically active sites and mass-transport pathways for the electrochemical reaction[91,92], and is therefore a crucial component of the system[93]. With the ongoing development of materials science and engineering[94], electrode modification has become an effective strategy for improving battery performance[95]. In ZFBs, dendrites tend to form readily on the anode during charging[96], making anode optimization particularly important[97]. Current electrode modification strategies mainly include bonding metal species to the substrate[98], constructing oriented graphene structures via electrospray[99], and related approaches.

Carbon materials, including graphene, carbon nanotubes, carbon fibers/carbon cloth, and porous carbon, are widely employed to modify and protect zinc metal anodes owing to their high electrical conductivity, abundant porosity, outstanding mechanical properties, and low cost. The high specific surface area of certain three-dimensional conductive substrates, such as carbon cloth, carbon felt, and graphene aerogels, substantially reduces the local current density, thereby delaying or suppressing the nucleation of zinc dendrites. Widely used as conductive current collectors and zinc storage hosts, these 3D carbon materials possess extensive internal pores that can accommodate the volume changes of zinc during repeated zinc deposition/dissolution cycles, thus mitigating macroscopic electrode deformation[100]. Moreover, some carbon materials have been doped with heteroatoms such as nitrogen, oxygen, sulfur, and phosphorus. These non-carbon atoms effectively induce local electronic rearrangement, creating strong "zincophilic active sites" that facilitate uniform nucleation of zinc ions, thereby avoiding the tip effect and guiding the oriented, smooth growth of zinc crystals along energetically stable crystallographic planes[101].

Finite element simulation shows that the in-plane pores of graphene can alleviate structural stress and inhibit dendrite growth by uniformly distributing zinc-ion flux across the material[102]. The formation of metal-substrate bonding at the electrode interface can increase the chemical potential for zinc nucleation, thereby

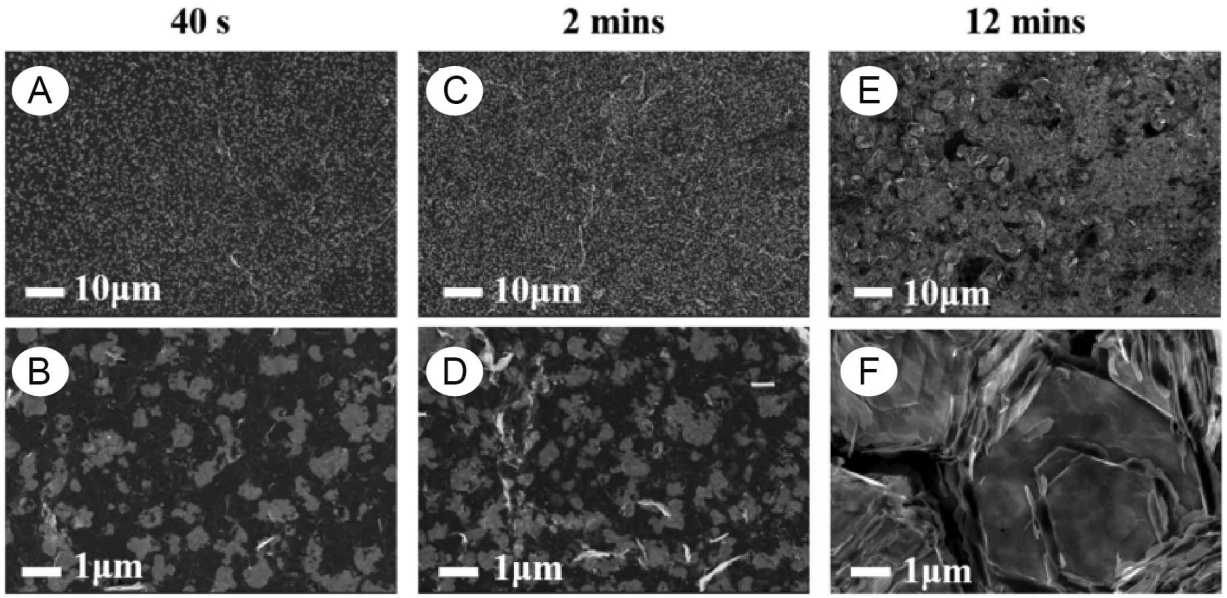

Figure 5. Scanning electron microscopy (SEM) of zinc deposits on graphene-coated stainless steel. Reprinted with permission from[98], Copyright 2019, The American Association for the Advancement of Science. SEM deposition times: (A and B) 40 s, (C and D) 2 min, and (E and F) 12 min. Current density: 4 mA cm^{-2}.

lowering the nucleation overpotential and promoting uniform zinc deposition[103]. During charging, forming an electrochemically inert interface with appropriate metal symmetry and lattice parameters can effectively facilitate heteroepitaxial nucleation of zinc in a nearly strain-free state, thereby suppressing disordered dendrite growth [Figure 5A-D]. Once the deposited zinc fully covers the three-dimensional carbon felt substrate, the subsequent deposition process gradually shifts from heteroepitaxy to homoepitaxy, leading to the formation of a uniform metal coating [Figure 5E and F]. Such an ordered interfacial structure provides an ideal epitaxial growth template for zinc deposition and enables highly reversible deposition/stripping behavior during cycling. At the anode, graphene-based electrodes can form Zn-graphene bonds, thereby precisely controlling the morphology of zinc deposition and suppressing parasitic side reactions. Epitaxial deposition of zinc yields substantial noticeable improvements in reversibility (CE > 99% over 1,000 cycles). The improvement could stem from the suppression of hydrogen evolution and other side reactions. In addition, constructing macro-textured substrates and preferentially exposing crystal planes with low lattice mismatch are beneficial for achieving large-area uniform epitaxial deposition. These strategies provide important guidance for the development of high-energy-density, long-lifespan ZFBs[98].

Another case of electrode modification for dendrite suppression involves leveraging electrostatic forces[104]. Given its large-scale applicability and cost, electrospray, a mature industrial technology, is singled out as a good candidate for 3D electrode interfacial engineering[99]. The electrostatic spraying deposition (ESD) technique can be used to construct a 3D porous reduced graphene oxide (rGO) coating on the surface of the zinc anode. The 3D porous rGO layer not only provides abundant channels for zinc-ion transport but also homogenizes the interfacial electric-field distribution, thereby effectively inhibiting dendrite growth and side reactions[105]. The deposition amount of graphene can be precisely controlled by adjusting the electrostatic spraying time and flow rate[106], thereby enabling the formation of thin-layer, highly aligned graphene structures[107]. Key steps include: (1) constructing a graphene-textured layer with consistent orientation on the macroscopic 3D structure surface via electrostatic spraying [Figure 6A], and (2) regulating interfacial Zn-C bonding, which stabilizes the electrode/electrolyte interface, effectively suppresses zinc dendrite growth and concurrently mitigates hydrogen evolution side reactions. This approach allows for long-term stability even under high areal capacity (25 mAh cm^{-2}) and high-power density (115 mW cm^{-2}) conditions. Compared

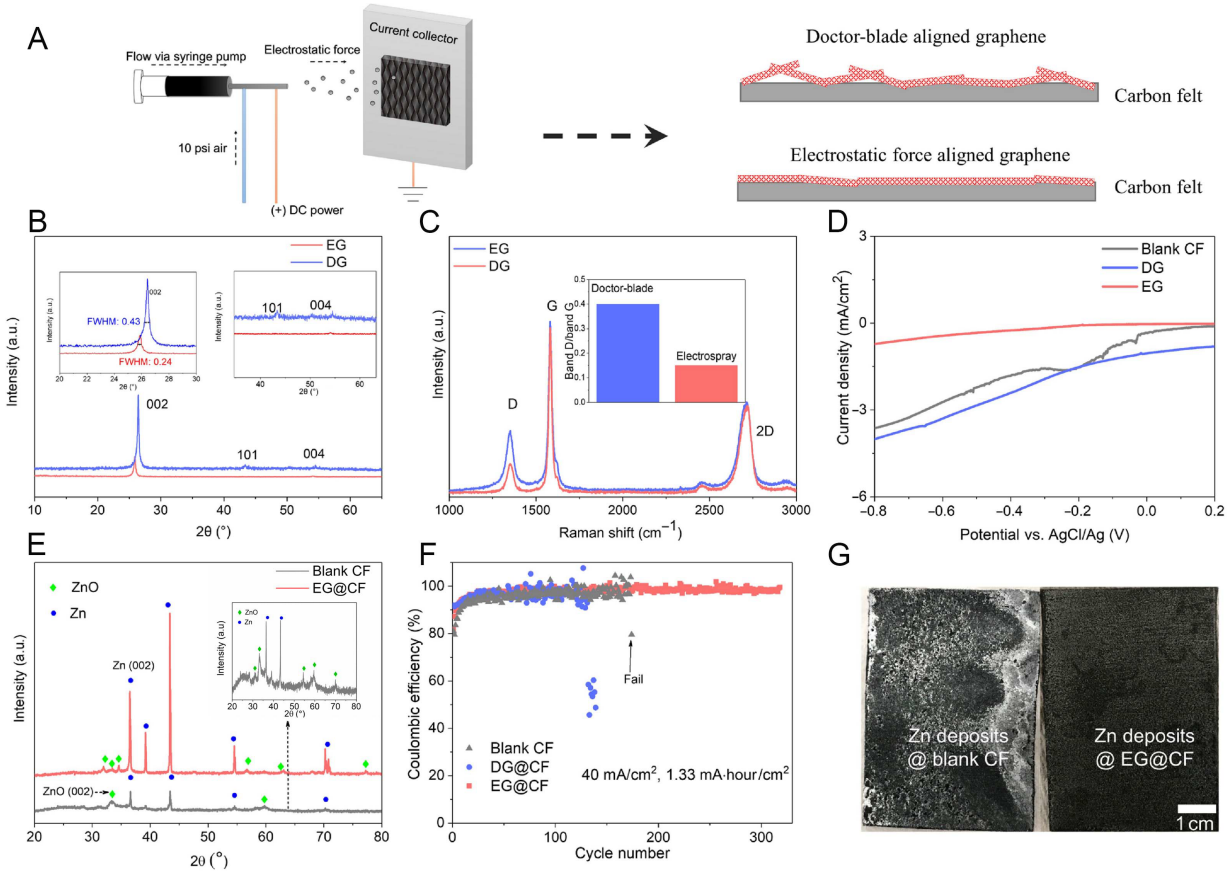

Figure 6. Interfacial designing for anode substrates. Reprinted with permission from[99], Copyright 2022, The American Association for the Advancement of Science. (A) Schematic illustrating the electrospray process used to manufacture textured graphene coatings, enabling reversible zinc electrodeposition. (B) X-ray diffraction (XRD) pattern of graphene coatings prepared via the standard doctor-blade (DG) method and the electrospray (EG) methodology. Inset: magnification of the (101) and (004) planes, highlighting the selectivity for crystallinity achieved by electrospray coatings. (C) Raman spectrum for graphene coatings fabricated by the doctor-blade and electrospray methods. Inset: D/G band intensity ratio. (D) Current density-potential curves illustrating variations in the HER current for blank carbon (CF), DG@CF, and EG@CF substrates. (E) XRD analysis of zinc deposits after cycling on blank CF and EG@CF. (F) CE of blank CF, DG@CF, and EG@CF. (G) Zinc deposition morphology on blank CF and EG@CF after 10 cycles at 40 mA cm^{-2}, 20 mAh cm^{-2}. *a. u.*: arbitrary units.

with graphene prepared via the doctor-blade shear method (DG), electrospray graphene (EG) exhibits superior performance. X-ray diffraction analysis shows that the EG layer primarily exposes the (002) plane [Figure 6B]. Raman spectroscopy indicates a reduced D/G band ratio, demonstrating improved alignment of the graphene layers under the electrostatic forces [Figure 6C]. Significantly, graphene aligned by electrostatic force can not only regulate the zinc electrodeposition but also lower the HER catalytic activity, which may result from less edge exposure since edge sites are generally regarded as catalytically active sites. The current density distribution of EG@CF is more uniform and orderly [Figure 6D]. After 20 cycles, the EG@CF surface exhibits less ZnO byproduct [Figure 6E], indicating suppressed hydrogen evolution. During discharge, zinc is stripped while the substrate remains intact, achieving a coulombic efficiency above 99.5% and stable cycling over 300 cycles, compared with the blank CF (98%, 150 cycles) and DG@CF (98.5%, 120 cycles) [Figure 6F]. Even at a larger scale, the EG@CF surface remains uniform and smooth [Figure 6G][99].

In summary, electrode modification plays a critical role in improving the performance and stability of ZFBs by regulating zinc nucleation, deposition morphology, and interfacial reactions. Strategies such as forming metal-substrate bonding and constructing epitaxially matched interfaces enhance the chemical potential for zinc nucleation, lower overpotentials, and promote uniform zinc deposition, effectively suppressing dendrite

growth. Graphene-based electrodes, whether integrated via lattice-matched interfaces or fabricated through electrostatic spraying, provide ordered epitaxial templates that stabilize the electrode-electrolyte interface, reduce parasitic side reactions, and enable highly reversible zinc deposition/stripping. Notably, electrospray graphene allows precise control over layer thickness and alignment, resulting in uniform current density distribution, suppressed HER, minimal ZnO byproduct formation, and exceptional cycling stability even under high areal capacity and power density conditions. Together, these approaches highlight the importance of tailored electrode design for achieving high-energy-density and long-lasting ZFBs and provide valuable guidance for future research on advanced zinc electrode architectures.

Separator design

In ZFBs, the function of the separator is to selectively allow the passage of specific ions[43] while maintaining electrical neutrality during operation[108]. However, the separators are prone to being pierced by zinc dendrites[38]. Current strategies for separator modification focus on simultaneously improving selectivity and conductivity by tuning pore structures[72], surface coating treatments[109], and chemical functionalization of the membrane surfaces[110]. Only a few researchers have attempted to design high-performance separators with dendrite-suppressing properties[38]. The structural and surface properties of the separator play a critical role in influencing zinc dendrite formation. The use of high-strength, microporous separators, such as modified cellulose or inorganic composite membranes, enables their robust frameworks to physically block dendrite penetration, effectively preventing internal short circuits within the battery[111,112]. In addition, coating or in situ growth of functional layers (e.g., metal oxides or carbon-based materials) on the separator surface introduces abundant zincophilic nucleation sites[113]. This not only reduces the local electric field intensity and mitigates the tip effect but also promotes uniform and smooth zinc deposition on the anode[114]. Furthermore, fine-tuning the surface chemistry of the separator to coordinate with Zn^{2+} preferentially can effectively repel or restrict water molecules from participating in electrode reactions, thereby suppressing hydrogen evolution and byproduct formation at their source[115].

Among the above-mentioned approaches, one effective method involves introducing negatively charged nanoporous membranes, such as PES/SPEEK membranes[110]. The sulfonic acid groups ($-SO_3^-$) on the membrane surface and pore walls generate strong electrostatic repulsion with zincate ions ($Zn(OH)_4^{2-}$) in the electrolyte [Figure 7]. This repulsion directs zincate ions away from the membrane interface during electrodeposition, promoting deposition toward the 3D carbon felt framework. Such a "reverse deposition" mechanism significantly reduces the risk of zinc dendrite penetration through the membrane. Even if dendrites form, they grow in the direction opposite to the membrane, preventing membrane damage and avoiding short circuits. Based on the above considerations, an alkaline zinc-iron flow battery with the membrane affords stable performance for about 240 cycles, free of zinc dendrite accumulation, at current densities ranging from 80 to 160 mA cm^{-2}. Furthermore, zinc deposited within the internal carbon felt structure forms a tightly integrated composite with the conductive framework, creating an effective carbon felt/metallic zinc composite electrode. This design enhances zinc utilization and cycle stability, mitigates polarization and capacity decay, and provides critical support for long-term operation of alkaline ZFBs[72].

In summary, separator modification is an effective strategy for suppressing zinc dendrite growth in ZFBs by regulating ion transport and deposition behavior. Conventional approaches, including pore structure tuning, surface coating, and chemical functionalization, can improve ion selectivity and mitigate active-species crossover. In particular, negatively charged nanoporous membranes such as PES/SPEEK membranes can electrostatically repel zincate ions, thereby inducing a "reverse deposition" mechanism in which zinc preferentially deposits within the 3D carbon felt framework rather than near the membrane surface. This not only reduces the risk of dendrite penetration and membrane damage, but also promotes the formation of a stable carbon felt/metallic zinc composite electrode, thereby enhancing zinc utilization, improving cycling stability, and reducing polarization and capacity decay.

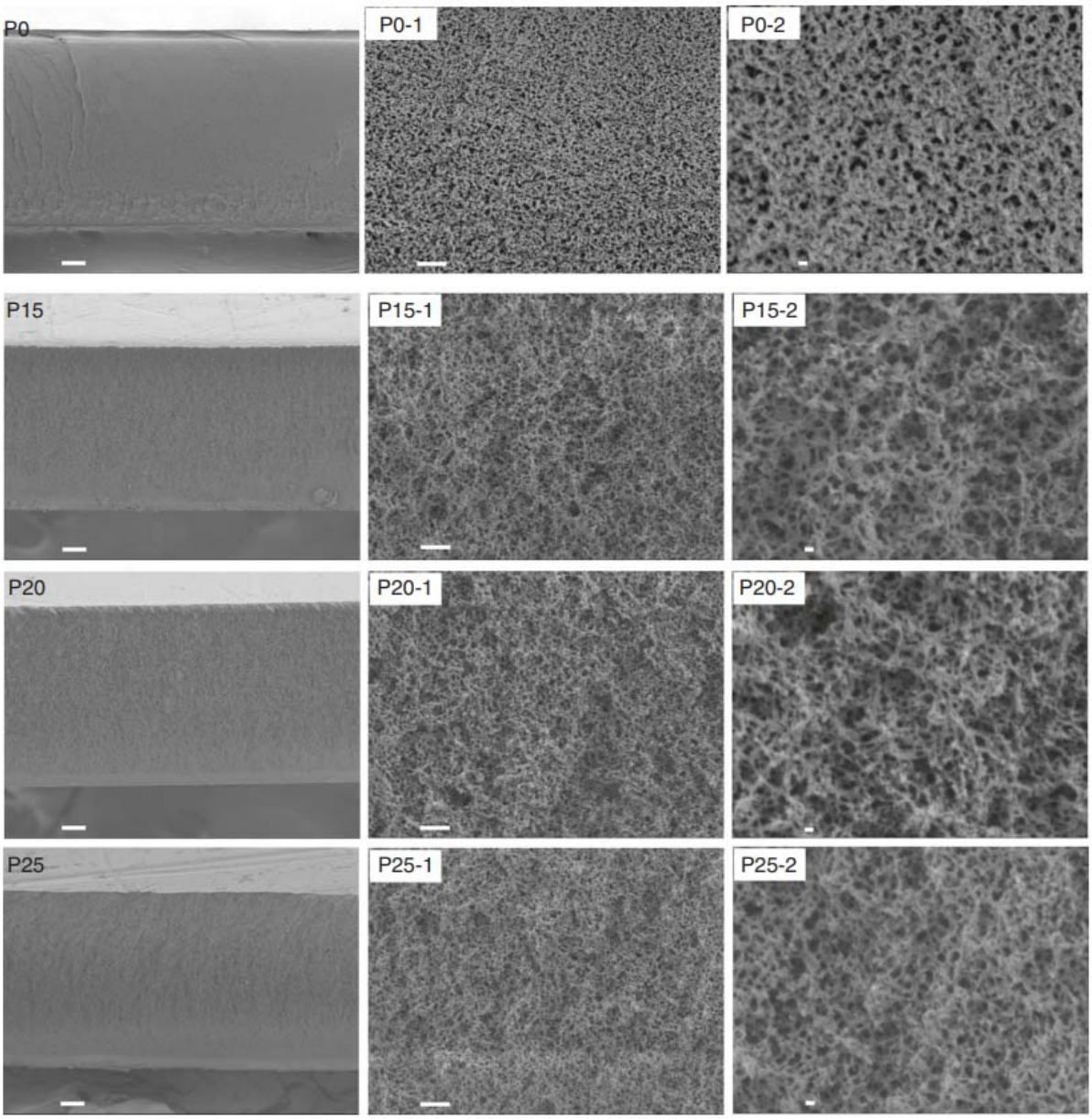

Figure 7. Cross-section morphologies of the PES/SPEEK membranes. Reprinted from Ref.[72]. In PX, X denotes the content of sulfonated poly(ether ether ketone) (SPEEK) in the polymer matrix; for instance, the P20 contains 20 wt% SPEEK. PX-1 and PX-2 show PX at different magnifications. The scale bars for PX, PX-1, and PX-2 are 10 μm, 1 μm, and 100 nm, respectively.

Operation regulation

In addition to the design strategies discussed above, critical operating parameters, including current density and flow rate, significantly influence zinc dendrite formation. Under real flow conditions, dendritic growth becomes more complex. Researchers have used multi-scale phase-field methods to study the formation, growth, and delamination of dendrites in ZFBs, systematically quantifying the conditions that trigger dendrite formation at low temperatures, low concentrations, low flow rates, and high current densities[116]. Research has shown that flowing electrolytes not only enhance ion convective transport but also suppress surface dendrite branching, thereby achieving a uniform distribution of concentration gradients and dense

deposition. Meanwhile, the flow of the electrolyte significantly suppressed the concentration overpotential, and charging under no-flow conditions will fail outright, demonstrating the differences between ZFBs and static aqueous zinc-ion batteries[117].

Theoretically, a sufficiently fast electrolyte flow can regulate the concentration distribution, thereby achieving uniform Zn deposition. Nevertheless, Ito *et al.* found that dendrite formation is not suppressed even at a high flow velocity of 15 cm s^{-1} during a 1 C charge, with the growth trajectory curving in the direction of the electrolyte stream[118]. Later studies reveal that Zn deposit morphology in flowing electrolyte is controlled by the ratio of applied current density to the diffusion-limited current density, which itself varies with flow rate and zinc salt concentration[119]. Xiao *et al.* employed a 3D model to simulate mass transport behavior in the flowing electrolyte. The results indicate that the near-electrode-surface flow velocity was close to zero, suggesting that concentration polarization cannot be eliminated in flow batteries[120]. From this perspective, increasing the flow rate improves Zn deposition uniformity, but it cannot fully eliminate dendrites, as dendrite growth also depends on current density and other operating conditions. Overall, a low current density, a low deposition capacity, and a high flow rate promote uniform zinc distribution, thereby reducing the formation of zinc dendrites. The current low zinc deposition area capacity is generally 20 mAh cm^{-2}, and the relatively low current density is 50 mA cm^{-2}[121].

At present, ZFBs have progressed from laboratory research to demonstration and pilot deployment. According to published reports, the U.S. Department of Energy has established a capital cost target of approximately \$150 kWh^{-1} for long-duration energy storage systems, along with a levelized cost of energy below \$0.10 kWh^{-1}, a round-trip efficiency exceeding 80%, and a cycle life greater than 5,000 cycles[122]. Since commercially available lithium iron phosphate batteries already meet these performance targets, ZFBs must achieve comparable metrics to demonstrate competitive engineering and economic viability[123]. Specifically, increasing the operating current density can enhance battery power density, thereby reducing stack size and associated capital costs[124]. Meanwhile, increasing the deposition areal capacity improves electrolyte utilization, thereby reducing electrolyte-related costs[125]. However, battery cost evaluation requires consideration of multiple factors, including the cathode material, battery chemistry, system configuration, charge-discharge power, and energy efficiency.

CONCLUSION AND OUTLOOK

In conclusion, zinc dendrite growth remains a major obstacle to the practical deployment of ZFBs because it undermines cycling stability, coulombic efficiency, and operational safety. Dendrite formation results from the combined effects of nonuniform electric fields, uneven ion transport, interfacial reaction heterogeneity, and parasitic side reactions, which promote localized zinc nucleation and self-amplifying growth. Considerable progress has been made through electrolyte engineering, anode modification, separator design, and operating-condition regulation. Although these strategies act through different mechanisms, they generally seek to homogenize zinc-ion transport and interfacial reactions while regulating zinc nucleation and growth. However, most approaches involve unavoidable trade-offs. Higher electrolyte flow rates reduce concentration polarization but increase pumping losses; thinner separators lower ohmic resistance but intensify active-species crossover; and protective additives can suppress dendrite growth and corrosion while increasing charge-transfer resistance. Therefore, dendrite-control strategies should be evaluated at the full-cell level, with balanced consideration of electrochemical performance, energy efficiency, durability, safety, and system cost.

Further progress requires a deeper understanding of dendrite evolution and greater emphasis on practical operating conditions. In particular, the effects of dendrite morphology, dead-zinc accumulation, and coupled side reactions on long-term battery performance remain insufficiently understood. Future research should

clarify the dynamic processes of zinc nucleation, growth, and dissolution under realistic electrolyte flow, current-density, and areal-capacity conditions; develop integrated strategies combining electrolyte, anode, separator, and operational regulation; establish standardized and reproducible testing protocols; and assess long-term stability, scalability, cost, and component compatibility. Addressing the interactions and trade-offs among different regulation methods will be essential for translating laboratory-scale improvements into reliable ZFB systems. With advances in mechanistic understanding, standardized evaluation, and application-oriented design, ZFBs could become a competitive technology for safe, low-cost, and large-scale energy storage.

DECLARATIONS

Authors' contributions

Conceptualization, writing - original draft: Jiang, Y.; Ren, J.
Writing - review and editing: Han, M.; Leung, P.; Li, Y.; Li, W.; Liu, B.; Jian, Q.; Zhang, J.
Funding acquisition, project administration: Wei, L.; Zhao, T.

Availability of data and materials

Not applicable.

AI and AI-assisted tools statement

Not applicable.

Financial support and sponsorship

This work was supported by Guangdong Major Project of Basic and Applied Basic Research (2023B0303000002), National Natural Science Foundation of China (No. 52576216, 12426307, 52536003), Guangdong Basic and Applied Basic Research Foundation (2023B1515120005, 2024A1515010288), Natural Science Foundation of Shenzhen (JCYJ20241202125327036, JCYJ20230807093315033), SUSTech Undergraduate Innovation and Entrepreneurship Training Program (YX202515), Commanding Heights of Science and Technology of Chinese Academy of Sciences (LDES150000), Research Project on Medium- and Long-Duration Flow Battery Energy Storage Technology (2024KJTW0015) and high-level of special funds (G03034K001).

Conflicts of interest

All authors declared that there are no conflicts of interest.

Ethical approval and consent to participate

Not applicable.

Consent for publication

Not applicable.

Copyright

© The Author(s) 2026.

REFERENCES

1. Zhao, M.; Cheng, T.; Li, T.; Wang, S.; Yin, Y.; Li, X. Molecular polarity regulation of polybromide complexes for high-performance low-temperature zinc-bromine flow batteries. *Energy. Environ. Sci.* **2025**, *18*, 378-85. DOI
2. Global energy review 2025. Washington: International Energy Agency; 2025.
3. Benitez, A.; Wulf, C.; Steubing, B.; Geldermann, J. Scenario-based LCA for assessing the future environmental impacts of wind offshore energy: an exemplary analysis for a 9.5-MW wind turbine in Germany. *Energ. Sustain. Soc.* **2024**, *14*, 49. DOI

4. Nguyen, V. D.; Ha, D. D.; Nguyen, T. H. T.; Nguyen, D. H. Generation expansion planning toward Net Zero target considering co-firing green fuel, CCUS installation and early decommissioning in thermal power plants: a case study of Vietnam. *AIMS. Energy.* . **2025**, *13*, 540-68. DOI
5. Hu, Y.; Min, Z.; Zhu, G.; et al. Predeposited lead nucleation sites enable a highly reversible zinc electrode for stable zinc-bromine flow batteries. *Nat. Commun.* **2025**, *16*, 3255. DOI PubMed PMC
6. Wei, Z.; Huang, Z.; Liang, G.; et al. Starch-mediated colloidal chemistry for highly reversible zinc-based polyiodide redox flow batteries. *Nat. Commun.* **2024**, *15*, 3841. DOI PubMed PMC
7. Beyers, I.; Krebeck, L.; Bensmann, A.; Hanke-Rauschenbach, R. Comparing operational flexibility and performance of pumped hydro energy storage systems: a quantitative analysis of technology options. *Energy. Convers. Manag. X.* **2026**, *29*, 101473. DOI
8. Ayoub, M.; Dincer, I. Energy and exergy analyses of an integrated thermal system with compressed air energy storage and carbon capture for power, cooling and domestic hot water applications. *Therm. Sci. Eng. Progs.* **2026**, *72*, 104586. DOI
9. Kityk, A.; Pavlik, V.; Hnatko, M. Integrating artificial intelligence with electrochemical science for advanced energy storage. *J. Energy. Storage.* **2026**, *150*, 120391. DOI
10. Ma, X.; Wu, D.; Wang, D.; et al. Optimizing pumped storage hydropower for multiple grid services. *J. Energy. Storage.* **2022**, *51*, 104440. DOI
11. Higashi, S.; Lee, S. W.; Lee, J. S.; Takechi, K.; Cui, Y. Avoiding short circuits from zinc metal dendrites in anode by backside-plating configuration. *Nat. Commun.* **2016**, *7*, 11801. DOI PubMed PMC
12. Chang, C.; Ye, X.; Li, X.; Tian, A.; Mei, F.; Jiang, J. Lithium-ion battery electrochemical-thermal-mechanical-impedance coupling model and voltage-impedance dual-objective parameter identification method. *J. Energy. Storage.* **2026**, *152*, 120748. DOI
13. Panda, M. R.; Gangwar, R.; Muthuraj, D.; et al. High performance lithium-ion batteries using layered 2H-$MoTe_2$ as anode. *Small* **2020**, *16*, 2002669. DOI
14. Zhou, Y.; Zhou, L.; You, Z.; et al. Progress in hard carbon anodes for sodium-ion batteries: storage mechanisms, precursors, and optimization strategies. *J. Energy. Storage.* **2025**, *138*, 118768. DOI
15. Gurkan, B. E.; Qiang, Z.; Chen, Y.; Zhu, Y.; Vogt, B. D. Enhanced cycle performance of quinone-based anodes for sodium ion batteries by attachment to ordered mesoporous carbon and use of ionic liquid electrolyte. *J. Electrochem. Soc.* **2017**, *164*, H5093-9. DOI
16. Lei, J.; Yao, Y.; Wang, Z.; Lu, Y. Towards high-areal-capacity aqueous zinc-manganese batteries: promoting MnO_2 dissolution by redox mediators. *Energy. Environ. Sci.* **2021**, *14*, 4418-26. DOI
17. Li, H.; Huang, B.; Chuai, M.; et al. Dual-plating aqueous Zn-iodine batteries enabled *via* halogen-complexation chemistry for large-scale energy storage. *Energy. Environ. Sci.* **2025**, *18*, 3160-8. DOI
18. Xie, C.; Liu, Y.; Lu, W.; Zhang, H.; Li, X. Highly stable zinc-iodine single flow batteries with super high energy density for stationary energy storage. *Energy. Environ. Sci.* **2019**, *12*, 1834-9. DOI
19. Cai, Y.; Zhang, H.; Wang, T.; et al. Directional regulation on single-molecule redox-targeting reaction in neutral zinc-iron flow batteries. *Joule* **2025**, *9*, 101768. DOI
20. Wang, Y.; Hong, H.; Wei, Z.; et al. Cation-regulated MnO_2 reduction reaction enabling long-term stable zinc-manganese flow batteries with high energy density. *Energy. Environ. Sci.* **2025**, *18*, 1524-32. DOI
21. Innocenti, A.; Bresser, D.; Garche, J.; Passerini, S. A critical discussion of the current availability of lithium and zinc for use in batteries. *Nat. Commun.* **2024**, *15*, 4068. DOI PubMed PMC
22. Rodby, K. E.; Jaffe, R. L.; Olivetti, E. A.; Brushett, F. R. Materials availability and supply chain considerations for vanadium in grid-scale redox flow batteries. *J. Power. Sources.* **2023**, *560*, 232605. DOI
23. Lourenssen, K.; Williams, J.; Ahmadpour, F.; Clemmer, R.; Gadsden, S. A.; Tasnim, S. H. Design, development, and testing of a low-concentration vanadium redox flow battery. *J. Electrochem. Energy. Convers. Storage.* **2021**, *18*, 011007. DOI
24. Zheng, H.; Ding, J.; Huang, J.; et al. Metal-organic frameworks facilitating complexation for long-cycle zinc-bromine flow batteries. *Adv. Funct. Mater.* **2025**, *36*, e14730. DOI
25. Iwakiri, I.; Antunes, T.; Almeida, H.; Sousa, J. P.; Figueira, R. B.; Mendes, A. Redox flow batteries: materials, design and prospects. *Energies* **2021**, *14*, 5643. DOI
26. Li, J.; Liu, W.; Chen, Y.; Wu, M. Temperature-dependent electrochemical dynamics in zinc-bromine flow batteries. *J. Energy. Storage.* **2026**, *166*, 122402. DOI
27. Khalid, M. Ed. Redox - principles and advanced applications. InTech. 2017. DOI
28. Zhao, Z.; He, Y.; Yu, W.; Shang, W.; Ma, Y.; Tan, P. Revealing the missing puzzle piece of concentration in regulating Zn electrodeposition. *Proc. Natl. Acad. Sci. USA.* **2023**, *120*, e2307847120. DOI PubMed PMC
29. Wei, Z.; Qu, G.; Huang, Z.; et al. Gradient distribution of zincophilic sites for stable aqueous zinc-based flow batteries with high capacity. *Adv. Mater.* **2024**, *36*, 2414388. DOI

30. Dai, H.; Sun, T.; Zhou, J.; et al. Unraveling chemical origins of dendrite formation in zinc-ion batteries via in situ/operando X-ray spectroscopy and imaging. *Nat. Commun.* **2024**, *15*, 8577. DOI PubMed PMC
31. Xia, W.; Xie, K.; Gao, S.; Song, Z.; Chen, L.; Li, C. Multidentate chelating ligands enable high-performance zinc-bromine flow batteries. *Angew. Chem. Int. Ed.* **2024**, *64*, e202418669. DOI
32. Zhao, R.; Lu, K.; Pasha, M.; Kuang, R.; Zhang, H.; Lu, S. Regulating the electrolyte network to accelerate reversible I^-/I_2Br^- conversion and suppress zinc dendrite formation in advanced zinc-iodine flow batteries. *J. Mater. Chem. A.* **2024**, *12*, 24468-76. DOI
33. Lee, J.; Kim, R.; Kim, S.; et al. Dendrite-free Zn electrodeposition triggered by interatomic orbital hybridization of Zn and single vacancy carbon defects for aqueous Zn-based flow batteries. *Energy. Environ. Sci.* **2020**, *13*, 2839-48. DOI
34. Guo, C.; Zhou, J.; Chen, Y.; et al. Synergistic manipulation of hydrogen evolution and zinc ion flux in metal-covalent organic frameworks for dendrite-free Zn-based aqueous batteries. *Angew. Chem. Int. Ed.* **2022**, *61*, e202210871. DOI
35. Xu, Z.; Wu, M. Toward Dendrite-free deposition in zinc-based flow batteries: status and prospects. *Batteries* **2022**, *8*, 117. DOI
36. Zhang, Y.; Hu, Y.; Dong, C.; et al. A Zn-dendrite dissolving membrane to increase the cycling life of zinc bromine flow batteries. *Adv. Funct. Mater.* **2025**, *36*, 2500909. DOI
37. Hu, Q.; Liu, Y.; Ding, Y.; et al. Microstructural engineering of zinc anodes: expediting the fabrication and industrial-scale deployment of high-performance batteries. *Mater. Sci. Eng. R. Rep.* **2026**, *169*, 101175. DOI
38. Lu, W.; Xie, C.; Zhang, H.; Li, X. Inhibition of zinc dendrite growth in zinc-based batteries. *ChemSusChem* **2018**, *11*, 3996-4006. DOI
39. Ling, R.; Zhu, Z.; Peng, K.; et al. Dual-function electrolyte additive design for long life alkaline zinc flow batteries. *Adv. Mater.* **2024**, *36*, 2404834. DOI
40. Kim, H.; Kang, S.; Kim, D.; et al. Electrolyte additives in zinc-based flow batteries: from molecular mechanisms to interfacial control. *ChemElectroChem* **2025**, *13*, e202500301. DOI
41. Zheng, X.; Liu, Z.; Sun, J.; et al. Constructing robust heterostructured interface for anode-free zinc batteries with ultrahigh capacities. *Nat. Commun.* **2023**, *14*, 76. DOI PubMed PMC
42. Li, W.; Dan, X.; Wen, Q.; et al. Enhanced CuZn coating on carbon fibers through C-O-Cu bridging bond for homogeneous zinc deposition in zinc-iron flow batteries. *Small* **2025**, *21*, 2505164. DOI
43. Yoopensuk, W.; Suppanucroa, N.; Pimoei, J.; et al. Optimizing ionic conductivity and ion selectivity in zinc-polyiodide flow batteries with composite polyamide-porous separators. *J. Energy. Storage.* **2024**, *86*, 111362. DOI
44. Nikumbe, D. Y.; Bavdane, P. P.; Bora, D.; Dave, V.; Bhatt, B.; Nagarale, R. K. Mitigation of dendrite growth in zinc-iodide flow battery with tröger's base anion exchange membrane. *J. Electrochem. Soc.* **2024**, *171*, 090519. DOI
45. Chen, H.; Kang, C.; Shang, E.; Liu, G.; Chen, D.; Yuan, Z. Montmorillonite-based separator enables a long-life alkaline zinc-iron flow battery. *Ind. Eng. Chem. Res.* **2022**, *62*, 676-84. DOI
46. Liu, Y.; Lu, X.; Lai, F.; et al. Rechargeable aqueous Zn-based energy storage devices. *Joule* **2021**, *5*, 2845-903. DOI
47. Yao, Y.; Lei, J.; Shi, Y.; Ai, F.; Lu, Y. Assessment methods and performance metrics for redox flow batteries. *Nat. Energy.* **2021**, *6*, 582-8. DOI
48. Lu, W.; Li, T.; Yuan, C.; Zhang, H.; Li, X. Advanced porous composite membrane with ability to regulate zinc deposition enables dendrite-free and high-areal capacity zinc-based flow battery. *Energy. Storage. Mater.* **2022**, *47*, 415-23. DOI
49. Jing, H.; Xing, H.; Zhang, H.; Du, X.; Wang, M.; Han, Y. Dynamics of zinc dendritic growth in aqueous zinc-based flow batteries: insights from phase field-Lattice-Boltzmann simulations. *Chem. Eng. J.* **2025**, *503*, 158318. DOI
50. Zhuang, Y.; Liang, Y.; Zhang, W.; et al. Rational electrolyte structure engineering for highly reversible zinc metal anode in aqueous batteries. *Nano. Micro. Lett.* **2026**, *18*, 102. DOI PubMed PMC
51. Hu, Z.; Zhang, F.; Zhou, A.; et al. Highly reversible Zn metal anodes enabled by increased nucleation overpotential. *Nano. Micro. Lett.* **2023**, *15*, 171. DOI PubMed PMC
52. Zou, Q.; Liang, Z.; Wang, W.; Dong, D.; Lu, Y. A nuclei-rich strategy for highly reversible dendrite-free zinc metal anodes. *Energy. Environ. Sci.* **2023**, *16*, 6026-34. DOI
53. Li, B.; Zhang, X.; Wang, T.; et al. Interfacial engineering strategy for high-performance Zn metal anodes. *Nano. Micro. Lett.* **2021**, *14*, 6. DOI PubMed PMC
54. Yu, D. In situ studies of Zn and ZnO growth kinetics during electrodeposition. Los Angeles: University of California; 2017. Available from: https://escholarship.org/uc/item/5ks8z974 [Last accessed on 21 Jul 2026].
55. Wang, K. Solutions for dendrite growth of electrodeposited zinc. *ACS. Omega.* **2020**, *5*, 10225-7. DOI PubMed PMC
56. Yin, Y.; Wang, S.; Zhang, Q.; et al. Dendrite-free zinc deposition induced by tin-modified multifunctional 3D host for stable zinc-based flow battery. *Adv. Mater.* **2019**, *32*, 1906803. DOI
57. Cao, L.; Li, D.; Deng, T.; Li, Q.; Wang, C. Hydrophobic organic-electrolyte-protected zinc anodes for aqueous zinc batteries. *Angew. Chem. Int. Ed.* **2020**, *59*, 19292-6. DOI

58. Xie, C.; Li, T.; Deng, C.; Song, Y.; Zhang, H.; Li, X. A highly reversible neutral zinc/manganese battery for stationary energy storage. *Energy. Environ. Sci.* **2020**, *13*, 135-43. DOI
59. Li, B.; Ma, Y.; Ma, J.; Chen, L.; Zhao, Y.; Tang, M. Challenges and opportunities facing zinc anodes for aqueous zinc-ion battery. *Energy. Mater. Devices.* **2024**, *2*, 9370044. DOI
60. Zhang, K.; Zhou, M.; Zhao, X.; et al. Unraveling cation-anion coupling via classic molecular dynamics and ab initio molecular dynamics simulation: design rules of organic additives for building fluorinated solid electrolyte interphase layer in zinc-ion batteries. *Future. Batteries.* **2026**, *9*, 100128. DOI
61. Yao, X.; Wang, Z.; Guo, J.; et al. Paschen-back effect modulation of SO_4^{2-} hydration in magnetized electrolyte toward dendrite-free Zn-ion batteries. *Nat. Commun.* **2025**, *16*, 5740. DOI PubMed PMC
62. Pan, C.; Lin, S.; Hwang, B.; Huang, W.; Lee, C. Stable Zn metal deposition/stripping in Zn-Li dual-ion batteries achieved by acetonitrile-water co-solvent enhanced acetamide-based deep eutectic electrolytes. *Future. Batteries.* **2025**, *7*, 100108. DOI
63. Zhao, H.; Zhang, Y.; Wang, H.; et al. Zincophilic surface engineering enables fast, reversible Zn plating/stripping for high-rate alkaline Zn-Fe flow batteries. *ACS. Sustain. Chem. Eng.* **2026**, *14*, 6999-7006. DOI
64. Jia, H.; Wang, Z.; Tawiah, B.; et al. Recent advances in zinc anodes for high-performance aqueous Zn-ion batteries. *Nano. Energy.* **2020**, *70*, 104523. DOI
65. Huang, S.; Li, M.; Song, Y.; et al. A universal coulombic efficiency compensation strategy for zinc-based flow batteries (Adv. Mater. 33/2024). *Adv. Mater.* **2024**, *36*, 2470265. DOI
66. Xiao, Y.; Wang, J. R.; Dai, S. J.; et al. Interface engineering of zinc anodes for zinc-based flow batteries. *Batter. Supercaps.* **2026**, *9*, e70290. DOI
67. Gao, H.; Wang, X.; Wu, M.; Sun, Z.; Nan, M.; Ma, X. Multi-functional electrolyte additive facilitating reversible and uniform zinc deposition for sustainable alkaline zinc-iron flow batteries. *J. Energy. Storage.* **2025**, *114*, 115942. DOI
68. Yang, Q.; Li, Q.; Liu, Z.; et al. Dendrites in Zn-based batteries. *Adv. Mater.* **2020**, *32*, 2001854. DOI
69. Fan, D.; Gong, J.; Deng, S.; Yan, H.; Zhu, Q.; Jiang, H. Progress and challenges of zinc-iodine flow batteries: from energy storage mechanism to key components. *J. Energy. Storage.* **2024**, *92*, 112215. DOI
70. Dong, D.; Wang, T.; Sun, Y.; Fan, J.; Lu, Y. Hydrotropic solubilization of zinc acetates for sustainable aqueous battery electrolytes. *Nat. Sustain.* **2023**, *6*, 1474-84. DOI
71. Cha, J. S.; Park, S.; Seo, N.; Kang, Y.; Lee, C.; Yang, J. H. Zincophilic CuO as electron sponge to facilitate dendrite-free zinc-based flow battery. *Nat. Commun.* **2025**, *16*, 844. DOI PubMed PMC
72. Yuan, Z.; Liu, X.; Xu, W.; Duan, Y.; Zhang, H.; Li, X. Negatively charged nanoporous membrane for a dendrite-free alkaline zinc-based flow battery with long cycle life. *Nat. Commun.* **2018**, *9*, 3731. DOI PubMed PMC
73. Huang, Y.; Wei, Z.; Yuan, Z.; Li, X. Oriented membranes with in-plane aligned nanosheets for high-energy-efficiency zinc-based flow batteries. *Mater. Horiz.* **2026**, *13*, 2489-97. DOI
74. Yuan, Z.; Yin, Y.; Xie, C.; Zhang, H.; Yao, Y.; Li, X. Advanced materials for zinc-based flow battery: development and challenge. *Adv. Mater.* **2019**, *31*, 1902025. DOI
75. Wei, X.; Cosimbescu, L.; Xu, W.; et al. Towards high-performance nonaqueous redox flow electrolyte via ionic modification of active species (Adv. Energy Mater. 1/2015). *Adv. Energy. Mater.* **2015**, *5*, 201570002. DOI
76. Zhang, S.; Wu, Y.; Gao, J.; et al. High-entropy electrolyte for scalable zinc-iodine flow batteries. *ACS. Energy. Lett.* **2026**, *11*, 2247-56. DOI
77. Wang, Z.; Yu, L.; Nie, Y.; Gao, A.; Xi, J. Neutral zinc-iron flow batteries: advances and challenges. *Small* **2025**, *21*, e09008. DOI
78. Alghamdi, N. S.; Rakov, D.; Peng, X.; et al. Tailoring Zn-ion solvation structures for enhanced durability and efficiency in zinc-bromine flow batteries. *Angew. Chem. Int. Ed.* **2025**, *64*, e202502739. DOI PubMed PMC
79. Hu, H.; Cheng, X.; Wang, J.; Xuan, T.; Wang, L. High-performance alkaline zinc flow batteries enabled by functional electrolyte additive containing nucleophilic groups. *Electrochim. Acta.* **2025**, *531*, 146434. DOI
80. Wang, C.; Gao, G.; Su, Y.; et al. High-voltage and dendrite-free zinc-iodine flow battery. *Nat. Commun.* **2024**, *15*, 6234. DOI PubMed PMC
81. Wang, S.; Yang, D.; Zhang, P.; et al. Liquid metal anode enables zinc-based flow batteries with ultrahigh areal capacity and ultralong duration. *Sci. Adv.* **2025**, *11*, eads3919. DOI PubMed PMC
82. Kaya, E.; Sonmez, F.; Kucukislamoglu, M.; Nebioglu, M. Selective anomeric deacetylation using zinc acetate as catalyst. *Chem. Pap.* **2012**, *66*, 312-5. DOI
83. Han, J.; Mariani, A.; Varzi, A.; Passerini, S. Green and low-cost acetate-based electrolytes for the highly reversible zinc anode. *J. Power. Sources.* **2021**, *485*, 229329. DOI
84. Vallet, V.; Wahlgren, U.; Grenthe, I. Chelate effect and thermodynamics of metal complex formation in solution: a quantum chemical study. *J. Am. Chem. Soc.* **2003**, *125*, 14941-50. DOI PubMed

85. Apelblat, A.; Manzurola, E. Solubilities of magnesium, calcium, barium, cobalt, nickel, copper, and zinc acetates in water from T = (278.15 to 348.15) K. *J. Chem. Thermodyn.* **1999**, *31*, 1347-57. DOI
86. Deacon, G. B.; Phillips, R. J. Relationships between the carbon-oxygen stretching frequencies of carboxylato complexes and the type of carboxylate coordination. *Coord. Chem. Rev.* **1980**, *33*, 227-50. DOI
87. Bai, P.; Li, J.; Brushett, F. R.; Bazant, M. Z. Transition of lithium growth mechanisms in liquid electrolytes. *Energy. Environ. Sci.* **2016**, *9*, 3221-9. DOI
88. Shen, Q.; Jiang, M.; Wang, R.; et al. Liquid metal-based soft, hermetic, and wireless-communicable seals for stretchable systems. *Science* **2023**, *379*, 488-93. DOI
89. Rahim, M. A.; Tang, J.; Christofferson, A. J.; et al. Low-temperature liquid platinum catalyst. *Nat. Chem.* **2022**, *14*, 935-41. DOI
90. Andrew Musgrave, C. S.; Lu, N.; Sato, R.; Nagai, K. Gallium-tin alloys as a low melting point liquid metal for repetition-pulse-laser-induced high energy density state toward compact pulse EUV sources. *RSC. Adv.* **2019**, *9*, 13927-32. DOI PubMed PMC
91. Liu, Y.; Xu, J.; Lu, S.; Xiang, Y. Titanium nitride nanorods array-decorated graphite felt as highly efficient negative electrode for iron-chromium redox flow battery. *Small* **2023**, *19*, 2300943. DOI
92. Wang, R.; Li, Y.; He, Y. Achieving gradient-pore-oriented graphite felt for vanadium redox flow batteries: meeting improved electrochemical activity and enhanced mass transport from nano- to micro-scale. *J. Mater. Chem. A.* **2019**, *7*, 10962-70. DOI
93. Mayr, A.; Liang, Y.; Hille, L.; Daub, R. A methodology for evaluating electrode interface quality through contact area analysis of calendering-induced particle indentations. *Powder. Technol.* **2026**, *472*, 122042. DOI
94. Dobrzański, L. A. Significance of materials science for the future development of societies. *J. Mater. Proc. Technol.* **2006**, *175*, 133-48. DOI
95. Kitamura, N.; Imura, T.; Ishida, N.; Ishibashi, C.; Idemoto, Y. Facile surface modification of $MgMn_2O_4$ positive-electrode material for improving cycle performance of magnesium rechargeable batteries. *ACS. Omega.* **2022**, *7*, 46915-21. DOI PubMed PMC
96. Li, C.; Xin, Y.; Gao, W.; Chen, Y. Enabling a robust long-life zinc-iodine flow battery by stabilizing the zinc anode in a halide-rich electrolyte. *Small* **2025**, *21*, e08359. DOI
97. Wang, Y.; Zhu, D.; Guo, T.; et al. Surface passivation of carbon felt stabilizes zinc anodes for membrane-free aqueous zinc-based flow batteries. *Mater. Today. Energy.* **2025**, *53*, 101999. DOI
98. Zheng, J.; Zhao, Q.; Tang, T.; et al. Reversible epitaxial electrodeposition of metals in battery anodes. *Science* **2019**, *366*, 645-8. DOI
99. Jin, S.; Shao, Y.; Gao, X.; et al. Designing interphases for practical aqueous zinc flow batteries with high power density and high areal capacity. *Sci. Adv.* **2022**, *8*, eabq4456. DOI PubMed PMC
100. Wang, P.; Peng, T.; Ban, Y.; Zheng, M. Hierarchical pore structure composite electrode by electrospinning for dendrite-free zinc-based flow battery. *Adv. Funct. Mater.* **2024**, *34*, 2409036. DOI
101. Wang, L.; Fan, G.; Liu, J.; et al. Selective nitrogen doping on carbon cloth to enhance the performance of zinc anode. *Chin. Chem. Lett.* **2021**, *32*, 1095-100. DOI
102. Zhou, Z.; Cao, L.; Li, L.; et al. Synergy of modulating in-plane pores and zincophilic sites on the flexible graphene paper for efficient and dendrite-free hosted Zn anode. *Mater. Today. Energy.* **2024**, *44*, 101606. DOI
103. Hull, C. M.; Switzer, J. A. Electrodeposited epitaxial Cu(100) on Si(100) and lift-off of single crystal-like Cu(100) foils. *ACS. Appl. Mater. Interfaces.* **2018**, *10*, 38596-602. DOI
104. Zhu, Z.; Zhang, T.; Chen, Z. Electrostatic shielding for stable, dendrite-free zinc anodes in rechargeable zinc-air batteries. *Colloids. Surf. A. Physicochem. Eng. Asp.* **2026**, *735*, 139530. DOI
105. Su, T.; Gull, S.; Lin, W.; et al. 3D porous reduced graphene oxide-coated zinc anodes for highly-stable aqueous zinc-ion capacitors via electrostatic spray deposition. *Carbon* **2024**, *229*, 119467. DOI
106. Yan, J.; Leng, Y.; Guo, Y.; et al. Highly conductive graphene paper with vertically aligned reduced graphene oxide sheets fabricated by improved electrospray deposition technique. *ACS. Appl. Mater. Interfaces.* **2019**, *11*, 10810-7. DOI
107. Zulkharnay, R.; Ualibek, O.; Toktarbaiuly, O.; May, P. W. Hydrophobic behaviour of reduced graphene oxide thin film fabricated via electrostatic spray deposition. *Bull. Mater. Sci.* **2021**, *44*, 112. DOI
108. Varshini, V.; Naresh, R.; Srinivasan, M. S.; Induja, S.; Vasudevan, S.; Ragupathy, P. Unveiling the power of filter paper reinforced polymer composite membrane in zinc-bromine redox flow battery applications. *J. Electrochem. Soc.* **2025**, *172*, 070502. DOI
109. Yuan, Z.; Zhu, X.; Li, M.; Lu, W.; Li, X.; Zhang, H. A highly ion-selective zeolite flake layer on porous membranes for flow battery applications. *Angew. Chem. Int. Ed.* **2016**, *55*, 3058-62. DOI
110. Xu, W.; Li, X.; Cao, J.; Yuan, Z.; Zhang, H. Morphology and performance of poly(ether sulfone)/sulfonated poly(ether ether ketone) blend porous membranes for vanadium flow battery application. *RSC. Adv.* **2014**, *4*, 40400-6. DOI
111. Ma, H.; Chen, H.; Liu, W.; et al. Coupling polyethyleneimine grafting with macropore filling in ultrathin cellulose separator to enable robust aqueous zinc-based batteries. *J. Energy. Chem.* **2026**, *114*, 826-34. DOI

112. Ogawa, S.; Takazawa, Y.; Harada, H.; Nogami, M. The development of the organic/inorganic composite separator for use in secondary zinc batteries. *Electrochemistry* **2022**, *90*, 017001-. DOI
113. Liu, Y.; Zhang, X.; Rong, J.; Li, D.; Lv, S.; Sun, X. TiO_2/CNF interlayer functional separator for aqueous zinc ion batteries. *J. Energy. Storage.* **2025**, *114*, 115886. DOI
114. Wu, G.; Yang, W.; Yang, Y.; Yang, H. Dendrite-free strategies for aqueous zinc-ion batteries: structure, electrolyte, and separator. *J. Electrochem.* **2024**, *30*, 2415003. DOI
115. Kim, S.; Ju, S.; An, G. Mechanically robust and water-trapping separators for zinc-ion batteries via hydrophilic surface engineering. *J. Energy. Chem.* **2025**, *111*, 237-48. DOI
116. Mushtaq, F.; Xiang, Y.; Fahim, M.; Xie, X.; Zhao, H.; Daoud, W. A. Untangling dendrite growth dynamics in hybrid flow batteries. *Energy. Storage. Mater.* **2024**, *73*, 103864. DOI
117. Tachida, Y.; Yamada, R.; Morimitsu, M. Polarization behaviors and morphology during zinc deposition and dissolution in zinc flow battery. *Meet. Abstr.* **2023**, *MA2023-02*, 2886. DOI
118. Ito, Y.; Nyce, M.; Plivelich, R.; Klein, M.; Steingart, D.; Banerjee, S. Zinc morphology in zinc-nickel flow assisted batteries and impact on performance. *J. Power. Sources.* **2011**, *196*, 2340-5. DOI
119. Ito, Y.; Wei, X.; Desai, D.; Steingart, D.; Banerjee, S. An indicator of zinc morphology transition in flowing alkaline electrolyte. *J. Power. Sources.* **2012**, *211*, 119-28. DOI
120. Xiao, M.; Wang, Y.; Yao, S.; Song, Y.; Cheng, J.; He, K. Analysis of internal reaction and mass transfer of zinc-nickel single flow battery. *J. Renew. Sustain. Energy.* **2016**, *8*, 064102. DOI
121. Huang, Y.; Zhi, L.; Bi, R.; Yuan, Z.; Li, X. Perspectives on zinc-based flow batteries. *Fundam. Res.* **2026**, *6*, 173-7. DOI PubMed PMC
122. U.S. Department of Energy; 2013. Grid Energy Storage December 2013. Available from: https://www.energy.gov/oe/articles/grid-energy-storage-december-2013 [Last accessed on 22 Jul 2026].
123. Liu, J.; Huang, Z.; Fan, M.; Yang, J.; Xiao, J.; Wang, Y. Future energy infrastructure, energy platform and energy storage. *Nano. Energy.* **2022**, *104*, 107915. DOI
124. Chen, Z.; Liu, Y.; Yu, W.; et al. Cost evaluation and sensitivity analysis of the alkaline zinc-iron flow battery system for large-scale energy storage applications. *J. Energy. Storage.* **2021**, *44*, 103327. DOI
125. Sun, X.; Wang, D.; Hu, H.; et al. Double-doped carbon-based electrodes with nitrogen and oxygen to boost the areal capacity of zinc-bromine flow batteries. *Trans. Tianjin. Univ.* **2024**, *30*, 74-89. DOI

Disclaimer/Publisher's Note: All statements, opinions, and data contained in this publication are solely those of the individual author(s) and contributor(s) and do not necessarily reflect those of OAE and/or the editor(s). OAE and/or the editor(s) disclaim any responsibility for harm to persons or property resulting from the use of any ideas, methods, instructions, or products mentioned in the content.

© The Author(s) 2026. Open Access This article is licensed under a Creative Commons Attribution 4.0 International License (https://creativecommons.org/licenses/by/4.0/), which permits unrestricted use, sharing, adaptation, distribution and reproduction in any medium or format, for any purpose, even commercially, as long as you give appropriate credit to the original author(s) and the source, provide a link to the Creative Commons license, and indicate if changes were made.